HHS Public Access

Author manuscript

Nat Cell Biol. Author manuscript; available in PMC 2016 April 01.

Published in final edited form as:

Nat Cell Biol. 2015 October ; 17(10): 1294–1303. doi:10.1038/ncb3229.

Lipid signalling couples translational surveillance to systemic detoxification in *Caenorhabditis elegans*

J. Amaranath Govindan[1,2], **Elamparithi Jayamani**[1,3], **Xinrui Zhang**[1], **Peter Breen**[1], **Jonah Larkins-Ford**[1], **Eleftherios Mylonakis**[3], and **Gary Ruvkun**[1,2]

[1]Department of Molecular Biology, Massachusetts General Hospital, Boston, MA 02114, USA

[2]Department of Genetics, Harvard Medical School, Boston, MA 02115, USA

[3]Division of Infectious Diseases, Rhode Island Hospital, Alpert Medical School of Brown University, Providence, RI 02903

Abstract

Translation in eukaryotes is surveilled to detect toxins and virulence factors and coupled to the induction of defense pathways. *C. elegans* germline-specific mutations in translation components are detected by this system to induce detoxification and immune responses in distinct somatic cells. An RNAi screen revealed gene inactivations that act at multiple steps in lipid biosynthetic and kinase pathways that act upstream of MAP kinase to mediate the systemic communication of translation-defects to induce detoxification genes. Mammalian bile acids can rescue the defect in detoxification gene induction caused by *C. elegans* lipid biosynthetic gene inactivations. Extracts prepared from *C. elegans* with translation deficits but not from wild type can also rescue detoxification gene induction in lipid biosynthetic defective strains. These eukaryotic antibacterial countermeasures are not ignored by bacteria: particular bacterial species suppress normal *C. elegans* detoxification responses to mutations in translation factors.

Introduction

Exposure of eukaryotes to chemical toxins induces the expression of detoxification enzymes and transporters that modify and excrete these xenobiotics[1]. Because inactivation by RNAi of genes that encode targets of natural toxins also induces detoxification responses, surveillance of the core cellular processes such as translation, electron transport, etc., rather than detection of toxins via their molecular signatures, may detect toxic and pathogen attacks and couple to the induction of defense responses[2]. Sentinel cells that detect xenobiotics could induce a protective systemic response. A prediction of this cellular

Correspondence to: Gary Ruvkun.

Author contributions

J.A.G. and G.R conceived the project. E.J. and E.M. provided the microbes used in the experiments. E.J. performed the bacterial suppression experiments. J.L.F. helped with the data collection and analysis. X.Z. conducted the qRT-PCR experiments. P.B. constructed transgenic pmk-1::mcherry lines. J.A.G. and G.R wrote the paper.

Competing financial interests

The authors declare no competing financial interests

surveillance model is that disruption of such core processes even by a host mutation in such components should be interpreted by this system as a toxic attack and cause induction of detoxification and immunity genes. Here, we report that a variety of mutation-induced defects that disrupt translation only in the *C. elegans* germline trigger the induction of detoxification and innate immune gene expression in the intestine, the organ most likely to encounter bacterial pathogens. Laser ablation of germline stem cells abrogates this xenobiotic response to germline translation-defective mutations, showing that germ cells are the signaling center. An RNAi screen for genes that are required for the induction of xenobiotic response genes after exposure to drugs that inhibit translation or in response to mutations that disable germline translation revealed a kinase cascade and a lipid biosynthetic pathway that generates systemic signals of impaired translation. Purified mammalian bile acids can rescue the signaling defects in the lipid biosynthetic gene-inactivated animals, suggesting that the signals of translational malaise are bile acid derivatives. Particular bacterial species from a panel that we tested can suppress these host surveillance and detoxification pathways, showing that these pathways are targets of bacterial modulation.

Results

Inactivation of *C. elegans* translation components by feeding the animals *E. coli* expressing specific dsRNAs targeting translation factor mRNAs induces the expression of xenobiotic detoxification genes, bacterial pathogen response genes, and aversion behavior[2–4] (Fig. 1a–c; Supplementary Tables 1–3). Toxins such as the eukaryotic translation inhibitors G418, produced by the bacteria *Micromonospora rhodorangea*[5], or hygromycin, produced by the soil bacteria *Streptomyces hygroscopicus*[6], also induce these responses. Detoxification responses in animals include cytochrome P450's (CYPs), UDP-glucuronosyltransferases (UGTs), glutathione S-transferases (GSTs), and p-glycoprotein transporters (PGPs) (Fig. 1a–e; Supplementary Tables 1–3). We chose a *pgp-5::gfp* fusion gene for assays of xenobiotic detoxification induction in response to G418, hygromycin, or ribosomal assaults via RNAi (Fig. 1a–e; Supplementary Tables 1–3) because of the robust response of this reporter gene and validation of this gene induction from microarray gene expression analysis in response to translational inhibition by toxins or RNAi[4].

Systemic surveillance of translational inhibition

To test whether a mutational defect in translation in a single tissue is interpreted similarly to induce a systemic xenobiotic and innate immune response, we crossed the *pgp-5::gfp* fusion gene into mutants that are defective for translation only in the germline[7]. Some of the genes that encode protein translation components are duplicated in *C. elegans*, with one gene dedicated to translation in the germline and the other gene to somatic cell translation[7]. For example, *C. elegans* bears two translation initiation factor eIF-5A orthologues, *iff-1* and *iff-2*, one specific to the germline and the other specific to somatic cells[8]. *iff-1* is expressed only in the germline, and is required for its growth and proliferation; an animal homozygous for an *iff-1* null allele is sterile due to a defect in germline translation, but has normal somatic *iff-2* function and grows to adulthood at a normal rate[8]. In contrast, an *iff-2* loss of function mutation is larval lethal[8]. Similarly, *eft-3* and *rpl-11.1* are required for translation in the germline while their duplicate genes *eft-4* and *rpl-11.2* mediate somatic cell translation[7].

Using GFP fusions to particular cytochrome p450 and ABC transporter detoxification genes, we observed high expression in the intestine in *iff-1(tm483)* homozygotes but almost no expression in *iff-1(tm483)*/+ heterozygous animals or wild type (Supplementary Fig. 1a). A GFP fusion to the innate immune response gene, *irg-1*, identified based on its strong response to the pathogen *Pseudomonas aeroginosa* PA14[3], was also activated in the *iff-1(tm483)* homozygous germline translation-defective mutant (Fig. 2a). Homozygous *eft-3(q145)* and *rpl-11.1(ar228)* sterile mutants also induced particular suites of detoxification genes, as assayed by RT-qPCR analysis or GFP fusion genes (Fig. 2a–d, and Supplementary Fig. 1b–c). Inactivation of the somatic homologues of these translation components also induced detoxification and innate immunity genes (Fig. 1a,b and Supplementary Fig. 1d). The germline translation mutation-induced xenobiotic defense response is not a general stress response because the mitochondrial stress response reporter gene *hsp-60::gfp* was not induced in the homozygous *eft-3(q145)* mutant (Supplementary Fig. 1e).

The translation-defective germline actively signals to the intestine to induce detoxification response genes; ablation of germ stem cells in *eft-3(q145) pgp-5::gfp* abrogated *pgp-5::gfp* induction in the intestine (Supplementary Fig. 1f–h). The systemic induction of detoxification by tissue-specific translation defects was not limited to the germline: tissue-specific translation deficits induced by RNAi in only muscle, neurons, hypodermis, using tissue-specific rescue of an *rde-1* RNAi defective mutant[2], can also induce a systemic detoxification in the intestine, showing that many cell types may be monitored by this system (Supplementary Fig. 1i,j).

To identify the signaling components that are required for induction of *pgp-5::gfp* or *gst-4::gfp* in the intestine in response to the *iff-1(tm483)* or *rpl-11.1(ar228)* germline-translation-defective mutations, we screened a 450-gene kinase and 600-gene transcription factor RNAi library (See Methods; Supplementary Tables 4,5). Positive hits from the screen were rescreened on the *eft-3(q145);pgp-5::gfp* germline translation-defective strain and most were required for *pgp-5::gfp* induction in *eft-3(q145)* (Fig. 3a,b). These gene inactivations also disrupted *pgp-5::gfp* or chromosomal *pgp-5* induction by the translation-inhibitory drugs hygromycin or G418 (Fig. 3c–e). Several kinases including *pmk-1*–p38 MAPK, and its known upstream kinases, as well as the *zip-2*–bZIP, and *skn-1*–Nrf transcription factors were required for the intestinal induction of detoxification genes in the germline translation mutants (Supplementary Tables 4 and 5; Fig. 3a–e).

Using an antibody to PMK-1–p38 MAPK protein to analyze which tissues activate PMK-1, as determined by its relocalization to the nucleus[9], we observed that the PMK-1 kinase is activated in the intestine of germline translation-defective mutants (Fig. 4a,b). This immunostaining was absent in *pmk-1(km25)* null mutant animals demonstrating the specificity of the antibody (Supplementary Fig. 2a–c). Transgenic animals that express mCherry-labeled PMK-1 protein in the intestine under the *vha-6* promoter confirmed the intestinal activation of PMK-1 observed with the antibody: mCherry-labeled PMK-1 protein was nuclearly-localized in *eft-3(q145);pmk-1(km25)* compared to *pmk-1(km25)* with similar levels of mCherry::PMK-1 expression (Supplementary Fig. 2d). Nuclear mCherry::PMK-1 in the intestine of *eft-3(q145);pmk-1(km25)* colocalized with the phospho-p38 antibody

staining, suggesting that the nuclear PMK-1 corresponds to activated PMK-1–p38 MAPK (Supplementary Fig. 2e). Because expression of p38 MAPK only in the intestine of the *eft-3(q145);pmk-1(km25)* mutant, missing PMK-1 in all other cells types, is sufficient to induce p38 MAPK activation and subsequent nuclear localization in the intestine, the PMK-1–p38 MAPK acts in the intestine to transduce the signal of germline translation defects to somatic xenobiotic response.

We monitored PMK-1 nuclear localization after gene inactivation of the other hits in the screen, to order them upstream or downstream of PMK-1 activation and nuclear localization. Inactivation of *prk-2* (Pim oncogene related kinase), *kin-18* (TAO1 kinase), *svh-2* (hepatocyte growth factor receptor related) and *mig-15* (Nck-interacting kinase) as well as the known upstream MAPK component *tir-1* caused decreased nuclear PMK-1 in the intestine of *eft-3(q145)* homozygotes (Fig. 4b), mapping these kinase activities upstream of PMK-1 nuclear relocalization. By contrast, RNAi of *zip-2* had no effect on PMK-1 nuclear relocalization in *eft-3(q145)* homozygotes (Fig. 4b), showing that the ZIP-2 transcription factor acts downstream or in parallel to this kinase cascade.

Genome-wide RNAi screen for translational surveillance regulators

A genome-wide RNAi screen identified 170 gene inactivations that disrupt *pgp-5::gfp* response to G418 (Supplementary table 8). We tested the 170 primary screen candidate gene inactivations in duplicate for disruption of *pgp-5::gfp* induction in *eft-3(q145)* homozgyous animals (Supplementary table 9); 71 gene inactivations also disrupted normal *pgp-5::gfp* induction in response to a germline translation defect (Supplementary table 9; Figure 4c–e). Inactivation of many of the genes from the RNAi screen caused hypersensitivity to G418 or hygromycin (Supplementary Fig. 2g, Fig. 4f,g), suggesting that when detoxification response is decoupled from the detection of translation defects, these drugs show increased potency. DAVID analysis revealed a strong enrichment of kinase signaling in this genome-wide screen, including the MAP kinase pathway implicated in innate immune responses[2,4] (Supplementary table 9) and several of the genes that identified in the kinase and transcription factor RNAi library screens (Supplementary Fig. 2f). In addition, multiple steps in a dual peroxisomal fatty acid or bile acid-like biosynthetic pathway disrupted *pgp-5::gfp* induction in response to *eft-3(q145)* germline translational defects, G418 or hygromycin (Supplementary table 9; Fig. 4d,e). For example, *daf-22* and *nlt-1* encode conserved protein domains contained in mammalian SCPx, which mediates bile acid and branched chain fatty acid metabolism[10,11] which are bisected into two *C. elegans* genes. Similarly, *dhs-28* encodes a protein that is orthologous to next upstream enzyme in the mammalian bile acid and branched chain fatty acid biosynthetic pathway, peroxisomal multifunctional protein 2[10,11].

Because the lipid–bile acid pathway could synthesize a small molecule endocrine signal of translational malaise that might be conserved between species, we studied this pathway in more detail. Using the nuclear localization of PMK-1 p38 MAPK as a molecular signature of its activation, we found that the lipid–bile acid signaling components are required for germline translation-defect activation of nuclear PMK-1–p38 MAPK in the intestine (Fig.

4h; Supplementary Fig. 2h). Thus, lipid signaling functions upstream of intestinal p38 MAPK signaling.

To explore the types of lipids that the *dhs-28, daf-22* pathway generates to regulate the induction of *pgp-5::gfp* expression in translation-defective animals, we tested whether defects in *dhs-28* or *daf-22*-mediated lipid–bile acid biosynthesis could be rescued for *pgp-5::gfp* induction by addition of purified mammalian bile acids (Supplementary Fig. 2i). Addition of bovine chenodeoxycholic acid or glycochenodeoxycholic acid partially rescued the defect in induction of *pgp-5::gfp* caused by the *C. elegans daf-22* or *dhs-28* lipid biosynthesis gene inactivations (Fig. 5a–b) but did not rescue the defect in induction of *pgp-5::gfp* caused by *tir-1* or *zip-2* (Fig. 5b). Deoxycholic acid weakly rescued but lithocholic acid did not rescue. Thus a bile acid product of the *daf-22* and *dhs-28* pathway is required for signaling translational malaise rather than other lipids. Treatment of wild type animals carrying *pgp-5::gfp* with these purified mammalian bile acids did not induce *pgp-5::gfp*, suggesting that the bile signal is not sufficient to signal ribosomal deficiency (Supplementary Fig. 3a,b). However addition of mammalian bile acids enhanced the induction of *pgp-5::gfp* in worms subjected to mild inhibition of translation via dilution of *rpl-7* RNAi (Supplementary Fig. 3c). Bile acid addition was sufficient to induce xenobiotic detoxification if the MAP kinase signaling was enhanced by a mutation in *vhp-1*, which encodes a phosphatase that negatively regulates the JNK and p38 MAPK[12,13] (Supplementary Fig. 3d). Thus both activation of PMK-1 MAPK signaling and production of the bile acids may be required for induction of detoxification response pathways. Bile acid treatment does not induce *hsp-4::gfp* (a ER stress response chaperone gene) or *gpdh-1::gfp* (osmotic stress response gene) (Supplementary Fig. 3e,f), showing that it is not a general stress inducer.

If bile acid-like signals are produced by *C. elegans* in response to ribosomal deficiency, we expected that a crude lipid extract from *C. elegans* with translation defects would induce or enhance induction of *pgp-5::gfp* in another animal. A lipid extract from translationally-disrupted *eft-4* RNAi treated-animals did not induce *pgp-5::gfp* in wild type animals but lipid extracts from these animals enhanced the response to mild inhibition of translation (Fig. 5C; Supplementary Fig. 3g,h). Lipid extracts from wild type animals did not show this activity (Fig. 5C). Lipid extracts from animals undergoing translational inhibition either by *iff-2 RNAi* or *rpl-7 RNAi* showed the same activity as *eft-4* RNAi extracts.

Lipid signalling mediates translational surveillance

C. elegans produces bile acid-like steroids [10,11] from nutritionally derived cholesterol. In addition to their role in bile acid biosynthesis, *daf-22* and *dhs-28* encode peroxisomal proteins that also mediate lipid modifications to a secreted dauer arrest pheromone[14]; however we found no evidence of a coupling of translation-defects to dauer pheromone production (Supplementary Fig. 3i). *C. elegans* bile-like dafachronic acids also act at the most downstream outputs of this endocrine system to regulate dauer arrest via the DAF-12 nuclear hormone receptor[15], but this pathway is distinct from the *daf-22, ntl-1*, and *dhs-28* pathway because inactivation of the *daf-12* nuclear hormone receptor gene or addition of

purified dafachronic acids does not affect *pgp-5::GFP* induction in response to ribosomal defects (Supplementary Fig. 3j).

Modulation of translational surveillance by bacterial species

If a microbial secondary metabolite or virulence factor targets the same surveillance and xenobiotic response gene pathways, host surveillance and response to translation deficits would be compromised, rendering other toxins or virulence factors more effective. We screened a diverse collection of bacterial species (Supplementary Table 6) for disruption of intestinal *pgp-5::gfp* induction by a germline translation mutation when these bacterial species were fed to the *eft-3(q145); pgp-5::gfp* strain. Three bacterial species out of 40 tested strongly suppressed the induction of *pgp-5::gfp* in the homozygous *eft-3(q145); pgp-5::gfp* strain: *Kocuria rhizophila, Alcaligenes spp.*, and *Paenibacillus spp.* (Fig. 6a,b; Supplementary Fig. 3k). *Kocuria spp* are human skin microflora[16–18]. *Kocuria rhizophila*[19,20] and *Alcaligenes spp*[21–23] are human opportunistic pathogens while *Paenibacillus spp.* is a soil bacteria[24–26] associated with root knot nematodes and suppresses their virulence on plants[27]. *Kocuria rhizophila* also suppresses detoxification responses as measured by qRT-PCR to monitor endogenous genes (Fig. 6c,d). Other *K. rhizophila* isolates or the closely related *K. kristinae* and *K. marina* also abrogated induction of *pgp-5::gfp* in the germline translation mutant animals but feeding on other close taxons, *K. rosea* or *Micrococcus luteus* did not disrupt *pgp-5* induction (Fig. 6b). The unfolded protein response was normal in *upr-1(zc6);hsp-4::gfp* animals grown on *Alcaligenes spp.*, *Paenibacillus spp.* or *Kocuria rhizophila*, as it is on *E. coli* (Supplementary Fig. 3l), suggesting that the suppression of the activation of *pgp-5::gfp* by these bacterial strains is a specific regulation of detoxification and immunity.

Heat-killed *Kocuria* spp. did not disrupt *pgp-5::gfp* induction, showing that it is not a nutritional insult to *C. elegans* (Supplementary Fig. 3m). Supernatants from stationary cultures of *Kocuria spp.* did not suppress *pgp-5::gfp* induction in the germline- translation-defective *C. elegans* mutant (Supplementary Fig. 3m), suggesting that no stable toxin or virulence factor is secreted into the growth media. While PMK-1 is nuclearly localized in intestinal nuclei of *eft-3(q145)* homozygous animals fed on *E.coli*, weak or no nuclear staining and a reduction in intestinal nuclear mCherry::PMK-1 was seen in *eft-3(q145)* homozygous animals fed on *K. rhizophila* (Fig. 6e,f; Supplementary Fig. 2d). These data suggest that *Kocuria* produces, for example, a virulence factor that is transferred to the *C. elegans* intestine to silence the response to germline translation defects upstream of the PMK-1 MAP kinase cascade.

Discussion

We have shown that mutations that disrupt translation in particular tissues are misapprehended as a bacterial attack by an innate immunity and detoxification system that responds with gene expression countermeasures to microbial toxins. The induction of this pathway by germline mutations in translation factor genes is a strong support for the hypothesis[2] that toxins and virulence factors are detected by their inhibition of core cellular machinery rather than by their chemical detection in the mixture of much more abundant

cellular biochemicals. This system of surveillance has some similarities to effector triggered immunity system of plant pathogens in that for both systems virulence factors are detected and an immune response ensues[28]. But effector triggered immunity posits a dedicated host protein receptor, such as the nucleotide-binding–leucine-rich-repeat proteins, for each virulence factor, whereas the cellular surveillance system monitors host cellular pathways in parallel for any inhibition by toxin or virulence factor[2]. This surveillance model has the advantage of using the toxicity to host pathways of a toxin, which may interact with high affinity with its conserved cellular target, as the sensitive detector and trigger for induction of detoxification and immunity.

The disruption of core cellular processes in specific tissues such as the germline induce xenobiotic defense response in distant unaffected tissues. This finding although analogous to the mitochondrial dysfunction-induced systemic stress response[29,30] or the systemic heat shock response[31] involves distinct set of xenobiotic detoxification genes and signaling pathways, suggesting that distinct cellular insults trigger distinct response pathways. While the intestine and skin are the most likely tissues to first encounter bacterial toxins and virulence factors, the germline is also subject to bacterial infection: *Wolbachia* infection of the germline is endemic across arthropods[32] as well as the nematode pathogen *Brugia malayi*[33].

While the MAP kinase pathway has a well-established role in pathogen defense, our screen shows that this pathway also surveils for small chemical toxins. In addition, we could order the action of newly identified genes, such as the bile acid signaling pathway genes and less studied kinases, such as the *kin-18* RIO1 kinase, upstream of the MAP kinase pathway genes. In mammals, RIO1 kinase binds to ribosomes where it mediates ribosomal assembly[34]; *kin-18*–RIO1 activity in ribosome assembly or on the mature ribosome where it remains bound may also play a role in translational surveillance signaling to the MAPK pathway.

Our screen for gene inactivations that disrupt this surveillance pathway revealed many hits in a *C. elegans* lipid biosynthetic pathway, suggesting that particular lipids constitute a major axis of toxin and bacterial pathogen signaling. The partial rescue of the signaling defects of gene inactivations such as *daf-22* and *dhs-28* with 95% pure mammalian chenodeoxycholic acid or glycochenodeoxycholic acid, supports the model that the *C. elegans* lipid signal is a bile acid. However, it is possible that other lipids in those 95% pure mammalian bile salts actually mediate the rescue. Mammalian bile acids are conventionally thought to aid digestion as emulsifiers of fat, but a role in various systemic endocrine hormone-like functions has emerged[35]. Bile acids in mammals are synthesized from cholesterol in the liver as primary bile acids and, significantly for our proposal that they constitute signals of microbial attack, are metabolized by particular mammalian gut microbes to secondary bile acids[36]. Bile acids in mammals regulate metabolic pathways by activation of Farnesoid X receptor as well as the G-protein-coupled receptor (GPCRs) such as TGR5[36,37]. The defect in xenobiotic responses that we observe after inactivation of the *C. elegans nhr-267* nuclear hormone receptor gene may be a homologous response to mammalian bile salt FXR responses, although *nhr-267* is not an FXR orthologue (Supplementary table 8&2). Conversely, mammalian bile acids detected by FXR and LXR

may be internal signals of bacterial attack that couple via these nuclear hormone receptors to systemic detoxification. In this sense, these nuclear hormone receptors do not surveil for the infinity of possible chemical and protein toxins with their ligand binding domains, only for internally generated bile acid or other signals of distress produced by the system of surveillance of core cellular machinery[2].

Our screen for bacterial activities that suppress xenobiotic surveillance found that 10% of the disparate bacterial strains tested suppressed xenobiotic detoxification responses to a *C. elegans* germline transation mutation. While this hit rate seems remarkably high, bacterial strains can each produce dozens of virulence factors and toxins, many of which have evolved to disrupt eukaryotic biology. So this screen may have tested hundreds of toxins and virulence factors, many under selection in bacteria for their anti-eukaryotic activities, for suppression of the *C. elegans* xenobiotic surveillance and detoxification system. The *Kocuria* antisurveillance activity was not found in taxonomically related bacteria and depends on continued contact with live bacteria, suggesting that a transferred protein virulence factor(s) rather than a stable secreted small molecule mediates the activity. The microbial modulation of animal surveillance of core cellular components has important implications for the behavior of pathogenic and commensal bacteria. It suggests that bacteria may produce drugs and transferred proteins that silence eukaryotic surveillance systems to in turn suppress eukaryotic countermeasures to toxins and virulence factors. The removal of such innate immunity silencing activities by disruptions of the microbiome with antibiotics for example could trigger stronger immune reactions including autoimmunity and inappropriate immune reaction to normally benign microbes or chemicals.

Materials and methods

N2 Bristol was the wildtype strain used.

The strains and mutant alleles used are in Supplementary Table 7.

RT-qPCR experiments

RNA was isolated using TRI Reagent (Sigma), followed by chloroform extraction and isopropanol precipitation. Briefly ~ 300 day 1 adults treated with or without drugs were collected. RNA was DNAase treated using the TURBO DNA-free kit (Applied Biosystems). cDNA was prepared using the First strand cDNA synthesis kit from Invitrogen. qRT-PCR was performed with an iCycler machine (Bio-Rad) using iQ SYBR Green Supermix (Bio-Rad). All reactions were done in triplicate and on at least 2–4 biological replicates. All the values are normalized to ama-1 as internal control as well as to the transcript levels in untreated wildtype.

Primer sequence include

pgp-5F: TGTTCGAGCACTTAACATGGA

pgp-5R: CCCTGAATTACAGCTCGTTTG

pgp-6F: CGTTGGAGACAACACGACAT

pgp-6R: CAAATGTCCAGTCGACACGC

cyp-34A9F:ATTCATGCCTGTTTGGGTGCTC

cyp-34A9R:GCATCCACAAAGTCTTCACCCT

cyp-35B1F:TGCTTCTGACCACATTTCTTGCTG

cyp-35B1R: CAGGAGGGAGAAAGCGATCTTTG

ama-1F: CGGTCAGAAAGGCTATCGAG

ama-1R: CCAACCTCCTGACGATTGAT

cyp-14A3F: CTGTTCTTGATTTCTGGCTTGCTGG

cyp-14A3R: GACAGCTTGTGTGTACGGCA

pgp-12F: TCGACTGAGGATGTCGGTTCCATTG

pgp-12R: CAATGATTCCTAAACCCGGCTGCG

mrp-1F: GCAACAATTCCAACATTCCGCAAG

mrp-1R: CTGCATATTGCACGAGGTCACCA

pgp-9F: CCGGTACACAAGCACAGTAGATC

pgp-9R: CTGCCGCCGGAATCTATTTGACA

pgp-14F: CGAGCGACCTACCCGCAAATTAC

pgp-14R: GCACAAATGGTTCCAATGAACAGG

cyp-35A2F: AAGTATCAAGACTACCACCAGGTCC

cyp-35A2R: GACATCTCTCATAACCGGCGCATG

cft-1F: AATTCTGGAAGTCTTTCGCTGGAG

cft-1R: CCATTTCCACGCTGTCTTCTCCAAC

pgp-4F: GCGATTGATCACCGACTCGC

pgp-4R: CAATTGGTGCCATACTCCAGC

pgp-3F: GTTCACTTATCCAACTCGCCCAG

pgp-3R: GCTTCCTCGATGTCTTGATCCGTG

pgp-7 F: GATTACACGACACCACTCATAGCTC

pgp-7 R: CATTCCGCGTTCATACTGCTCATA

cyp25A1F: GGTTTAACGAGCTTCACGAGCAG

cyp25A1R: CAGATCGTGTATGCTTCCAACCA

cyp13A11F: TTATTCTCAGCTCAAGGCCATCG

cyp13A11R: CCATTGCTATGCGTCCAATCACGT

cyp44A1F: ACATTCTCCGAAATTCCTGGTCC

cyp44A1R: GCAGACGATACCATTCAGGACCATT

cyp13A7F: AGTCAAAGGGCCTAGAGGTCTAC

cyp13A7R: CTTCCATCTATGGCCTTGAGCAG

cyp14A1F: AGATGAAGCAAACGGGAAATCCTGG

cyp14A1R: GACATTGATGGCAAACGTGCTG

cyp34A8F: CGGGTCAGGAGACCACATCTAC

cyp34A8R: CTGGTACGGGCTGACTATCAATCGT

cyp13A5F: TTGGAAGCGGTTGAGAACTCTG

cyp13A5R: CGAAGGCTGGTTGTATAGATGGGAA

pgp-8F: GATTTCGAGAGGCGTTCAACG

pgp-8R: GAAGCAAGTGTCCAGCTTGT

pgp-10F: AGCTGATGGCGATGGGTCTG

pgp-10R: CATCGCAATCGACAGTCCCAA

K08D8.5F: ATGCTACCGAATGCTTTTCC

K08D8.5R: TCCTTGGGTGTAGTTTCCAA

F35E12.5F: ACACAATCATTTGCGATGGA

F35E12.5R: GGTAGTCATTGGAGCCGAAA

gst-38F: TCCAATGCTCGAGGTAGATGGCAA

gst-38R: ACGAGCCTCCGCGTAATAGTCTTT

clec-85 F: GTCTTTGGTCAATGCACACG

clec-85 R: CGACTGAGCATCCGTAAACT

clec-5 F: GCTGCTGAGAGCAAATGTAC

clec-5 R: CCATAGGAGGGAAACTGAACTG

F08G5.6F: TGGACAACCCAGATATGCAA

F08G5.6R: GTATGCGATGGAAATGGACA

pmp-4F: TTTGTGGCTCAACTTGAAGG

pmp-4R: GCTAATCCCAGGTAAGACTCA

haf-2F: ACAGTGAGGGATACGGAAAC

haf-2R: CCACAGTACGAGAGAAGACG

Haf-7F: AAGGAGCTGAATACGAGAGG

Haf-7R: GCACTGAGCACAATTTGACA

Abt-4F: CTGTCGCGGCATACATAAAG

Abt-4R: GAGTCGGATTGTGTAGGTGA

F49F1.6F: CTTGTGGAATATGCCATCAG

F49F1.6R: GGGCATTGTATCTTAACAGC

T28D8.5F: GTCGACTCAAGACCATCATGC

T28D8.5R: GAGTATCGGTAACGCAGACACC

Generation of pvha-6::mCherry::pmk-1 transgenic worms

pvha-6::mcherry:pmk-1::tbb-2 3′UTR was constructed in the pCFJ151 (MosSCI ttTi5605) vector backbone using the Gibson Isothermal Assembly method using the following primers:

ZED1: GTGCGCGCGATGCATTCGAAGATCTGCCCAGATATTGCCAGCATGCTCAACGTTG

ZED2: TATATGATCCATTGTTGTCTGTGGAAACATCTTATACAATTCATCCATGCCACCTGTC

ZED3: CGACAGGTGGCATGGATGAATTGTATAAGATGTTTCCACAGACAACAATGGATC

ZED4: GAAGGGAATGCTTGAAAGGATCTTGCATCTACGATTCCATTTTCTCCTCATCTTCC

ZED5: GAAGATGAGGAGAAAATGGAATCGTAGATGCAAGATCCTTTCAAGCATTCCC

ZED6: ATCTTACTTGCACTTATAATACGACTCATGATCCACGATCTGGAAGATTTCCAAC

The resultant result plasmid were injected into the wildtype worms at 5 ng/ml concentration along with myo-2::NLSgfp co-injection marker to generate transgenic extrachromosomal array worms.

Drug treatment

G418 (GoldBio) or hygromycin (GoldBio) was diluted in M9 to the desired concentration and added onto preseeded OP50 *E.coli* bacteria containing NGM plates. The plates were dried uncovered in the hood for at least 1 hour before seeding the worms. Synchronized L1-stage animals were dropped onto the drug containing plates and scored later. For drug resistance assays synchronized L1 larval stage animals of the appropriate genotype were fed with either control RNAi or with RNAi clones targeting bile acid biosynthetic pathways until they reach day two of adulthood. Subsequently, the RNAi-treated animals were egg-

prepped to obtain synchronized L1 larvae. ~100 L1 larvae were added to the plates containing G418. 100nM of Δ^4-Dafachronic Acid or (25S)-Δ^7-Dafachronic Acid from Cayman Chemical were used in the daf-12 experiments. In the purified bile experiments, bile from bovine and ovine (Mixed bile acids), chenodeoxycholic acids, glycochenodeoxycholic acid, glycocholic acid, taurocholic acid, lithocholic acid, and taurochenodeoxycholic acid from Sigma were diluted in M9 to the desired concentration (100μM) and added onto preseeded OP50 *E.coli* bacteria containing NGM plates. The plates were dried uncovered in the hood for at least 1 hour before seeding the worms.

Screen methods used for identifying genetic pathways that mediate translation mutant-induced xenobiotic defense response

For the kinase and transcription factor cherry picked library primary screen, *iff-1(tm483)*/+ ; *pgp-5::gfp* heterozygous adults were fed on RNAi-media containing plates seeded with *E. coli* expressing dsRNA corresponding to a *C. elegans* kinase or transcription factor gene and screened for whether the ¼ of the progeny of the genotype *iff-1(tm483)*/*iff-1(tm483); pgp-5::gfp* show decreased *pgp-5::gfp* expression compared to no gene inactivation control animals. Scoring for GFP induction was done only on *iff-1(tm483)/ iff-1(tm483)* homozygotes, which could be scored using absence of fluorescence from an RFP fusion gene integrated on the balancer chromosome. The screen was conducted at 22°C. Secondary screens on kinase or transcription factor hits from the *iff-1(tm483)*/*iff-1(tm483); pgp-5::gfp* initial screen were similarly done on the *eft-3(q145);pgp-5::gfp* strain. The cherry-picked libraries included mostly transcription factors and kinases libraries but they also included some genes annotated to act in the kinase pathways that are not actually kinases (such as tir-1). The screen for identifying genes required for *rpl-11.1(ar228)* germline translation-inhibition induced *gst-4::gfp* activation was conducted by feeding *rpl-11.1(ar228)*/+ ; *gst-4::gfp* heterozygous adults on RNAi-media containing plates seeded with *E. coli* expressing dsRNA corresponding to a *C. elegans* kinase or transcription factor gene and screened for whether the ¼ of the progeny of the genotype *rpl-11.1(ar228)*/ *rpl-11.1(ar228); gst-4::gfp* show decreased *gfp* expression visually compared to no gene inactivation control animals. Scoring for GFP induction was done only on *rpl-11.1(ar228)*/ *rpl-11.1(ar228)* homozygotes, which could be scored using another dominant Unc marker from the balancer chromosome.

Staining of dissected intestine and gonad

Germline and intestine were dissected in M9 using 22-gauge hypodermic needles by cutting either near the pharynx or the tail region. The germline and intestine are released from the worm because of pressure and were separated from the worm carcass. The dissected germline and intestine were fixed with 1% formaldehyde in M9 for 10 min and subsequently fixed in ice-cold methanol for 5 min at room temperature. The dissected germline and intestine were washed three times by centrifugation at 2000 RPM for 1 minute with 1X PBS containing 0.1% Tween 20 (PBST). Following the fixation, the dissected germline and intestine were blocked with PBST containing 1mg/ml BSA for one hour at room temperature. After blocking, the dissected germline and intestine were stained with Anti-ACTIVE® p38 pAb, Rabbit, (pTGpY) from Promega (Catalog no: V1211) diluted 1:1000 in PBST containing 1mg/ml BSA for 2 hour at room temperature. The dissected germline and

intestine were washed three times in PBST and then stained with Goat Anti-Rabbit IgG (Catalog no:111-165-144) secondary antibody from Jackson Research diluted in 1:1000 in PBST containing 1mg/ml BSA for 2 hour at room temperature. The dissected germline and intestine were washed three times in PBST and then mounted on 2% agarose pad on glass slide with Vectashield® containing DAPI (Catalog no: H-1200) from Vector Labs for imaging. For staining the pmk-1::mcherry transgenic worms, the worms were dissected, fixed and blocked as above. The dissected intestine was incubated with Living Colors® mCherry Monoclonal Antibody from Clontech (Catalog no:v 632543), and Anti-ACTIVE® p38 pAb, Rabbit, (pTGpY) from Promega (Catalog no: V1211) diluted 1:2000 and 1:1000 respectively in PBST containing 1mg/ml BSA for 2 hours. Following the incubation, the dissected intestine was washed three times in PBST and stained with Anti-mouse IgG (Catalog no: 515165-003) and Anti-Rabbit IgG (Catalog no: 111-095-144) secondary antibodies from Jackson Research diluted to 1:1000 in PBST containing 1mg/ml BSA for 2 hour at room temperature. The dissected intestine was washed three times in PBST and then mounted on 2% agarose pad on glass slide with Vectashield containing DAPI from Vector Labs for imaging.

Microscopy

Nematodes were mounted onto agarose pads and images were taken using a Zeiss AXIO Imager Z1 microscope fitted with a Zeiss AxioCam HRm camera and Axiovision 4.6 (Zeiss) software. Fluorescent images were converted to 16-bit images, thresholded and quantified using ImageJ. Student's t test and ANOVA was used determine statistical significance.

Genome-wide RNAi screen

RNAi bacteria expressing the dsRNA corresponding to each worm gene were grown in LB media with 25μg/ml carbenicillin overnight and seeded onto RNAi agar plates containing 1mM IPTG. The following RNAi libraries were used for screening: Ahringer RNAi library, Vidal supplemental RNAi clone library and the new supplemental clones RNAi Library from Source Bioscience. The plates were allowed to dry in a laminar flow hood and incubated at room temperature overnight to induce dsRNA expression. 20 synchronized L1 larvae *pgp-5::gfp* expressing animals were placed onto RNAi-containing agar plates, allowed to develop at 15°C for 3 days to the L4-stage when 0.3 mg/ml of G418 in M9 was added to each RNAi well. The plates were allowed to dry in a laminar flow hood and incubated at 20°C. In the primary screen, the plates were screened visually for changes in GFP fluorescence and worm developmental defects. Any RNAi clones that caused lethality or decreased size or dramatically slowed development were excluded from the analysis. All the positive clones were retested at least twice and the clones were verified by DNA sequencing. The 170 hits from the G418 screen were also tested on the *iff-1(tm483)*/ *iff-1(tm483); pgp-5::gfp* and the *eft-3(q145);pgp-5::gfp* strains; 71 gene inactivations also disrupted activation of pgp-5 by these germline translation factor gene mutations. DAVID analysis was done on the 170 hits from the primary screen as well as on the 71 hits from the secondary screen with the germline translation defective mutation. From this analysis of the full genome screen, kinases were by far the most enriched, at a probability of 10^{-17}. Wormbase version WS247 was used to assign gene names to the hits.

Lipid extract preparation

A lipid extraction protocol[14] was used with the following modifications. Bleach-prepared embryos from wildtype were allowed to hatch without bacterial food and then fed from the L1-stage until adulthood in benign dsRNA control RNAi bacteria, *eft-4 RNAi*, *iff-1 RNAi* and *rpl-7 RNAi* bacteria on 60 large RNAi plates at 22°C. These worms were washed off the plates and resuspended in M9. The worms were washed at least three times to remove the bacteria. Subsequently, the worms were allowed to settle and the supernatant was removed. 5 ml of packed worms were lyophilized separately and kept at −80°C until use. The worm pellets were powdered in 0.1 M NaCl and liquid nitrogen using a mortar. The powdered pellets were extracted with 95% ethanol at 22°C for 24 h. The extracts were filtered using Whatman GF/A glass filter and were evaporated to dryness and resuspended in methanol.

Coculturing *pgp-5::gfp* animals with *eft-3(q145)* worms to test for animal to animal signaling of ribosomal stress

~2000 L1-larval stage *eft-3(q145)* homozygotes were sorted onto a 10cm NGM plate preseeded with *E.coli* OP50 using COPAS Biosorter®. ~100 L1-larval stage *pgp-5::gfp* worms were subsequently dropped onto the same plate and incubated at 20°C for 60 hours. The *pgp-5::gfp* worms on the plate were differentiated from the *eft-3(q145)* homozygotes on the basis of fertility. The fertile *pgp-5::gfp* worms on the plate was scored visually for *pgp-5::gfp* induction. In another experimental trial, the worms were sorted onto 10-cm plates seeded with dead OP50 instead of live *E.coli* OP50. In a third experimental trial, the worms were sorted onto 3-cm plates seeded with dead OP50 instead of live *E.coli* OP50. In a fourth experimental trial, the different concentrations (10–100 μm) of mixed bile acids were added to the worms were sorted onto 3-cm plates seeded with dead OP50. In all the cases, the fertile *pgp-5::gfp* worms on the plate was scored visually for *pgp-5::gfp* induction. We did not find any evidence for GFP induction in the non-*eft-3* mutant animals. The result of one such experiment is shown in Supplementary figure 3I.

Testing for non-specific effects of bile acids

Synchronized L1-larval stage *hsp-4::gfp* transgenic animals were grown to L4-larval stage at 20°C and treated with 1 μg/ml of DTT alone or with chenodeoxycholic acid 100μM for 24 hours. In experimental trials we also used DTT concentration renging from 1 to 7.5 μg/ml with and without different concentrations of mixed bile acids. In all cases, we did not observe induction of *hsp-4::gfp* or disruption of DTT induction of *hsp-4::gfp* by bile acids. One such experiment is shown in Supplementary figure 3e. In this experiment, synchronized L1-larval stage *hsp-4::gfp* transgenic worms were grown to L4-larval stage at 20°C and treated with 1 μg/ml of DTT alone or with chenodeoxycholic acid 100μM for 24 hours and imaged. 10 μg/ml of DTT induces *hsp-4::gfp* expression and it was used as positive control.

Growth and handling of microbes used

16S ribosomal sequence was amplified using 16S-specific primers and sequenced to identify the microbes. Brain Heart Infusion media as well as plates were used for culturing and testing the effect of *Enterococcus faecalis* and *E. faecium* on worms. For *Sacchromyces boulardi*, YPD media was used for growing the yeast and a concentrated culture was added

to SK media. For *Lactobacillus spp*, Lactobacilli broth was used for growing and then a concentrated culture was added to SK media. SK media was used for all the other microbes.

RT-qPCR experiments with worms fed on *Kocuria*

For the RT-PCR experiments involving *Kocuria*, synchronized L1-larval stage wildtype or *eft-3(q145)* homozygotes were fed on *E.coli* OP50 until L3-larval stage. The worms were subsequently washed several times in M9 to remove the adhering *E.coli* and then the worms were dropped onto SK medium plates containing either *E.coli* OP50 or *Kocuria*. The plates were incubated at 20°C for 40 hours and the worms were washed off the plates using M9. Following several washes to remove the bacteria, the worms were resuspended in M9. ~ 300 worms were used to isolate RNA using TRI Reagent (Sigma), followed by chloroform extraction and isopropanol precipitation. RNA was DNAase treated using the TURBO DNA-free kit (Applied Biosystems). cDNA was prepared using the First strand cDNA synthesis kit from Invitrogen. qRT-PCR was performed with an iCycler machine (Bio-Rad) using iQ SYBR Green Supermix (Bio-Rad). All reactions were done in triplicate and on at least 2–4 biological replicates. All the values are normalized to ama-1 as internal control as well as to the transcript levels in untreated wildtype. The Primer sequences used are given above.

Preparation of *Kocuria* extracts

K.rhizophila was grown in LB media for 5 days at 37°C and the culture were centrifuged at 4000 RPM for 20 min at 4°C. The supernatant was passed through a 0.45micron filter twice and the eluate was collected. 400µl of the eluate was added to 10-cm preseeded OP50 *E.coli* bacteria containing NGM plates. After the liquid has evaporated, ~100 L1-larval stage *eft-3(q145);pgp-5::gfp*–germline translation defective mutant worms were added to the plates and incubated at 20°C. When the worms reached adult stage (~60 hours after seeding onto plates), they were scored visually for the *pgp-5::gfp* induction. Supernatants prepared from OP50 grown in LB media using the same protocol mentioned above was used as control.

Preparation of heat-inactivated *Kocuria*

For preparing heat killed *K.rhizophila*, 5 ml overnight culture of *K.rhizophila* grown in LB media was centrifuged at 4000 RPM for 20 min at 4°C. The supernatant was removed and the pelleted bacteria were resuspended in 1 ml of M9. 500µl of the bacteria was heat inactivated at 70°C for 2 hours while the rest was used as control. 100 µl of the heat-inactivated culture was streaked onto LB media plates to ensure that bacteria are inviable. Following heat inactivation, 200 µl bacteria were seeded onto SK-media plates, dried and ~100 L1-larval stage *eft-3(q145);pgp-5::gfp*–germline translation defective mutant worms were added to the plates and incubated at 20°C. When the worms reached adult stage (~60 hours after seeding onto plates), they were scored visually for the *pgp-5::gfp* induction. 200 µl bacteria of the control non heat-inactivated bacteria prepared above were used as controls.

Phospho-PMK-1 activation staining assay with worms fed on *Kocuria*

Synchronized L1-larval stage wildtype or *eft-3(q145)* homozygotes were fed on *E.coli* OP50 until L3-larval stage. The worms were subsequently washed several times in M9 to remove the adhering *E.coli* and then the worms were dropped onto SK medium plates seeded with either *E.coli* OP50 or *Kocuria*. The plates were incubated at 20°C for 40 hours and ~100 worms were picked onto glass dish containing M9. The intestine of the worms was dissected in M9 using 22-gauge hypodermic needles by cutting either near the pharynx or tail region. The intestine is released from the worm because of pressure and is gently separated from the worm carcass. The dissected intestine was fixed with 1% paraformaldehyde in M9 for 10 min and subsequently fixed in ice-cold methanol for 5 min at room temperature. The dissected intestine was washed three times by centrifugation at 2000 RPM for 1 minute with 1X PBS containing 0.1% Tween 20 (PBST). Following the fixation, the dissected intestine was blocked with PBST containing 1mg/ml BSA for one hour at room temperature. After blocking, the intestine was stained with Anti-ACTIVE® p38 pAb, Rabbit, (pTGpY) from Promega (Catalog no: V1211) was diluted 1:1000 in PBST containing 1mg/ml BSA for 2 hour at room temperature. The dissected intestine was washed three times in PBST and then stained with Goat Anti-Rabbit IgG (Catalog no:111-165-144) secondary antibody from Jackson Research diluted in 1:1000 in PBST containing 1mg/ml BSA for 2 hour at room temperature. The intestine was washed three times in PBST and then mounted on 2% agarose pad on glass slide with Vectashield® containing DAPI from Vector Labs for imaging.

PMK-1 nuclear localization assay with worms fed on *Kocuria*

Synchronized L1-larval stage *pmk-1::mCherry* carrying transgenic worms or *eft-3(q145); pmk-1::mCherry* carrying transgenic worms and were fed on *E.coli* OP50 until L3-larval stage. The worms were subsequently washed several times in M9 to remove the adhering *E.coli* and then the worms were dropped onto SK medium plates seeded with either *E.coli* OP50 or *Kocuria*. The plates were incubated at 20°C for 40 hours. The worms were mounted onto 1% agarose pads and imaged using a Zeiss AXIO Imager Z1 microscope fitted with a Zeiss AxioCam HRm camera and Axiovision 4.6 (Zeiss) software.

Kocuria feeding suppresses *pgp-5::gfp* activation in response to germline translation inhibition

Synchronized L1-larval stage *eft-3(q145); pgp-5::gfp* worms were fed on *E.coli* OP50 until L3-larval stage. The worms were subsequently washed several times in M9 to remove the adhering *E.coli* and then the worms were dropped onto SK medium plates seeded with either *E.coli* OP50 or *Kocuria*. The plates were incubated at 20°C for 40 hours. The worms were mounted onto 1% agarose pads and imaged using a Zeiss AXIO Imager Z1 microscope fitted with a Zeiss AxioCam HRm camera and Axiovision 4.6 (Zeiss) software. Similar experimental procedure was used to test other *Kocuria* species and *Micrococcus luteus*.

Supplementary Material

Refer to Web version on PubMed Central for supplementary material.

Acknowledgments

Strains were provided by the Caenorhabditis Genetics Center (CGC), which is funded by NIH Office of Research Infrastructure Programs (P40 OD010440), and Shohei Mitani of the Japanese National Bioresources Project. This work was supported in part by the National Institutes of Health Grant AG043184-16A (to G.R.). Thanks to David Coil and Jonathan Eisen for providing *Kocuria* species.

References

1. Xu CC, Li CYTC, Kong ANTA. Induction of phase I, II and III drug metabolism/transport by xenobiotics. Arch Pharm Res. 2005; 28:249–268. [PubMed: 15832810]
2. Melo JA, Ruvkun G. Inactivation of conserved C. elegans genes engages pathogen- and xenobiotic-associated defenses. Cell. 2012; 149:452–466. [PubMed: 22500807]
3. Dunbar TLT, Yan ZZ, Balla KMK, Smelkinson MGM, Troemel EREC. elegans detects pathogen-induced translational inhibition to activate immune signaling. Cell Host Microbe. 2012; 11:375–386. [PubMed: 22520465]
4. McEwan DLD, Kirienko NVN, Ausubel FMF. Host translational inhibition by Pseudomonas aeruginosa Exotoxin A Triggers an immune response in Caenorhabditis elegans. Cell Host Microbe. 2012; 11:364–374. [PubMed: 22520464]
5. Waitz JA, Sabatelli F, Menzel F, Moss EL. Biological activity of antibiotic G-418, a new micromonospora-produced aminoglycoside with activity against protozoa and helminths. Antimicrob Agents Chemother. 1974; 6:579–581. [PubMed: 15825308]
6. Pittenger RC, Wolfe RN, Hoehn PN, Daily WA, McGuire JM. Hygromycin. I. Preliminary studies on the production and biologic activity of a new antibiotic. Antibiot Chemother (Northfield Ill). 1953; 3:1268–1278.
7. Maciejowski JJ, et al. Autosomal genes of autosomal/X-linked duplicated gene pairs and germ-line proliferation in Caenorhabditis elegans. Genetics. 2005; 169:1997–2011. [PubMed: 15687263]
8. Hanazawa M, et al. The Caenorhabditis elegans eukaryotic initiation factor 5A homologue, IFF-1, is required for germ cell proliferation, gametogenesis and localization of the P-granule component PGL-1. Mech Dev. 2004; 121:213–224. [PubMed: 15003625]
9. Mertenskötter A, Keshet A, Gerke P, Paul RJ. The p38 MAPK PMK-1 shows heat-induced nuclear translocation, supports chaperone expression, and affects the heat tolerance of Caenorhabditis elegans. Cell Stress Chaperones. 2013; 18:293–306. [PubMed: 23117578]
10. Ferdinandusse S, et al. Mutations in the gene encoding peroxisomal sterol carrier protein X (SCPx) cause leukencephalopathy with dystonia and motor neuropathy. Am J Hum Genet. 2006; 78:1046–1052. [PubMed: 16685654]
11. Autio KJ, et al. Role of AMACR (α-methylacyl-CoA racemase) and MFE-1 (peroxisomal multifunctional enzyme-1) in bile acid synthesis in mice. Biochem J. 2014; 461:125–135. [PubMed: 24735479]
12. Kim DH, et al. Integration of Caenorhabditis elegans MAPK pathways mediating immunity and stress resistance by MEK-1 MAPK kinase and VHP-1 MAPK phosphatase. Proc Natl Acad Sci U S A. 2004; 101:10990–10994. [PubMed: 15256594]
13. Mizuno T, et al. The Caenorhabditis elegans MAPK phosphatase VHP-1 mediates a novel JNK-like signaling pathway in stress response. EMBO J. 2004; 23:2226–2234. [PubMed: 15116070]
14. Butcher RA, et al. Biosynthesis of the Caenorhabditis elegans dauer pheromone. Proc Natl Acad Sci U S A. 2009; 106:1875–1879. [PubMed: 19174521]
15. Motola DL, et al. Identification of ligands for DAF-12 that govern dauer formation and reproduction in C. elegans. Cell. 2006; 124:1209–1223. [PubMed: 16529801]
16. Grice EA, et al. A diversity profile of the human skin microbiota. Genome Res. 2008; 18:1043–1050. [PubMed: 18502944]
17. Hillion M, et al. Comparative study of normal and sensitive skin aerobic bacterial populations. Microbiologyopen. 2013; 2:953–961. [PubMed: 24151137]
18. Zeeuwen PL, et al. Microbiome dynamics of human epidermis following skin barrier disruption. Genome Biol. 2012; 13:R101. [PubMed: 23153041]

19. Becker K, et al. Kocuria rhizophila adds to the emerging spectrum of micrococcal species involved in human infections. J Clin Microbiol. 2008; 46:3537–3539. [PubMed: 18614658]
20. Moissenet D, et al. Persistent bloodstream infection with Kocuria rhizophila related to a damaged central catheter. J Clin Microbiol. 2012; 50:1495–1498. [PubMed: 22259211]
21. Azzopardi EAE, Azzopardi SMS, Boyce DED, Dickson WAW. Emerging gram-negative infections in burn wounds. J Burn Care Res. 2011; 32:570–576. [PubMed: 21792068]
22. Obata T, Goto Y, Kunisawa J, Sato S. Indigenous opportunistic bacteria inhabit mammalian gut-associated lymphoid tissues and share a mucosal antibody-mediated symbiosis. Proc Natl Acad Sci U S A. 2010; 107:7419–7424. [PubMed: 20360558]
23. Sonnenberg GF, et al. Innate Lymphoid Cells Promote Anatomical Containment of Lymphoid-Resident Commensal Bacteria. Science. 2012; 336:1321–1325. [PubMed: 22674331]
24. Enright MR, Griffin CT. Specificity of Association between Paenibacillus spp. and the Entomopathogenic Nematodes, Heterorhabditis spp. Microb Ecol. 2004; 48:414–423. [PubMed: 15692861]
25. Montalvo-Katz S, Huang H, Appel MD. Association with Soil Bacteria Enhances p38-Dependent Infection Resistance in Caenorhabditis elegans. Infect Immun. 2013; 81:514–520. [PubMed: 23230286]
26. Zhang R, Hou A. Host-Microbe Interactions in Caenorhabditis elegans. ISRN microbiol. 2013; 2013:356451. [PubMed: 23984180]
27. Son SH, Khan Z, Kim SG, Kim YH. Plant growth-promoting rhizobacteria, Paenibacillus polymyxa and Paenibacillus lentimorbus suppress disease complex caused by root-knot nematode and fusarium wilt fungus. J Appl Microbiol. 2009; 107:524–532. [PubMed: 19457027]
28. Stuart LM, Paquette N, Boyer L. Effector-triggered versus pattern-triggered immunity: how animals sense pathogens. Nat Rev Immunol. 2013; 13:199–206. [PubMed: 23411798]
29. Durieux J, Wolff S, Dillin A. The cell-non-autonomous nature of electron transport chain-mediated longevity. Cell. 2011; 144:79–91. [PubMed: 21215371]
30. Liu Y, Samuel BS, Breen PC, Ruvkun G. Caenorhabditis elegans pathways that surveil and defend mitochondria. Nature. 2014; 508:406–410. [PubMed: 24695221]
31. Prahlad V, Cornelius T, Morimoto RI. Regulation of the cellular heat shock response in Caenorhabditis elegans by thermosensory neurons. Science. 2008; 320:811–814. [PubMed: 18467592]
32. Saridaki A, Bourtzis K. Wolbachia: more than just a bug in insects genitals. Curr Opin Microbiol. 2010; 13:67–72. [PubMed: 20036185]
33. Fenn K, Blaxter M. Wolbachia genomes: revealing the biology of parasitism and mutualism. Trends Parasitol. 2006; 22:60–65. [PubMed: 16406333]
34. Widmann B, et al. The kinase activity of human Rio1 is required for final steps of cytoplasmic maturation of 40S subunits. Mol Biol Cell. 2012; 23:22–35. [PubMed: 22072790]
35. Thomas C, Pellicciari R, Pruzanski M, Auwerx J, Schoonjans K. Targeting bile-acid signalling for metabolic diseases. Nat Rev Drug Discov. 2008; 7:678–693. [PubMed: 18670431]
36. Ridlon JM, Kang DJ, Hylemon PB. Bile salt biotransformations by human intestinal bacteria. J Lipid Res. 2006; 47:241–259. [PubMed: 16299351]
37. Kawamata Y, et al. A G protein-coupled receptor responsive to bile acids. J Biol Chem. 2003; 278:9435–9440. [PubMed: 12524422]

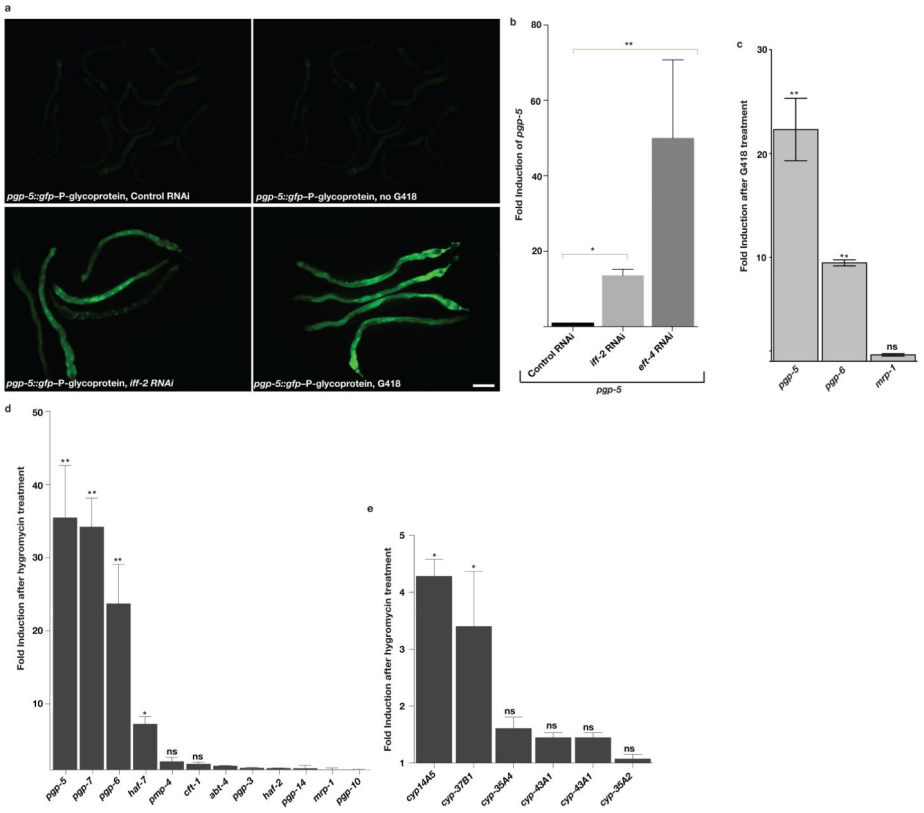

Figure 1. Translation inhibition using toxin or RNAi induces xenobiotic detoxification

A) The toxin G418 or inhibition of translation by *iff-2*(translation initiation factor) RNAi induces *pgp-5::gfp* expression in the intestine as assessed using a transcriptional promoter fusion. Scale bar, 50μm.

B) RNAi of translation initiation factor (*iff-2*) or elongation factor (*eft-4*) induces *pgp-5* mRNA as assessed by qRT-PCR. Fold change compared to control RNAi treated wildtype animals. **P<0.01.

C) G418 induces *pgp-5* and *pgp-6* mRNA from the chromosomal locus but not *mrp-1*– multidrug resistance protein homolog mRNA as assessed by qRT-PCR. Fold change compared to non-toxin-treated wildtype animals.

D) Hygromycin induces expression of particular xenobiotic efflux pump genes as assessed by qRT-PCR. Fold change compared to non-hygromycin-treated wildtype animals.

E) Hygromycin induces expression of particular xenobiotic detoxification genes as assessed by qRT-PCR. Fold change compared to no hygromycin-treated wildtype animals. B, C, D and E: Unpaired t test; **P<0.01, *P<0.05. ns; no significant difference. ~300 worms per condition were washed off 1 plate for each experiment. Mean ± s.d from n= 3 independent experiments is shown.

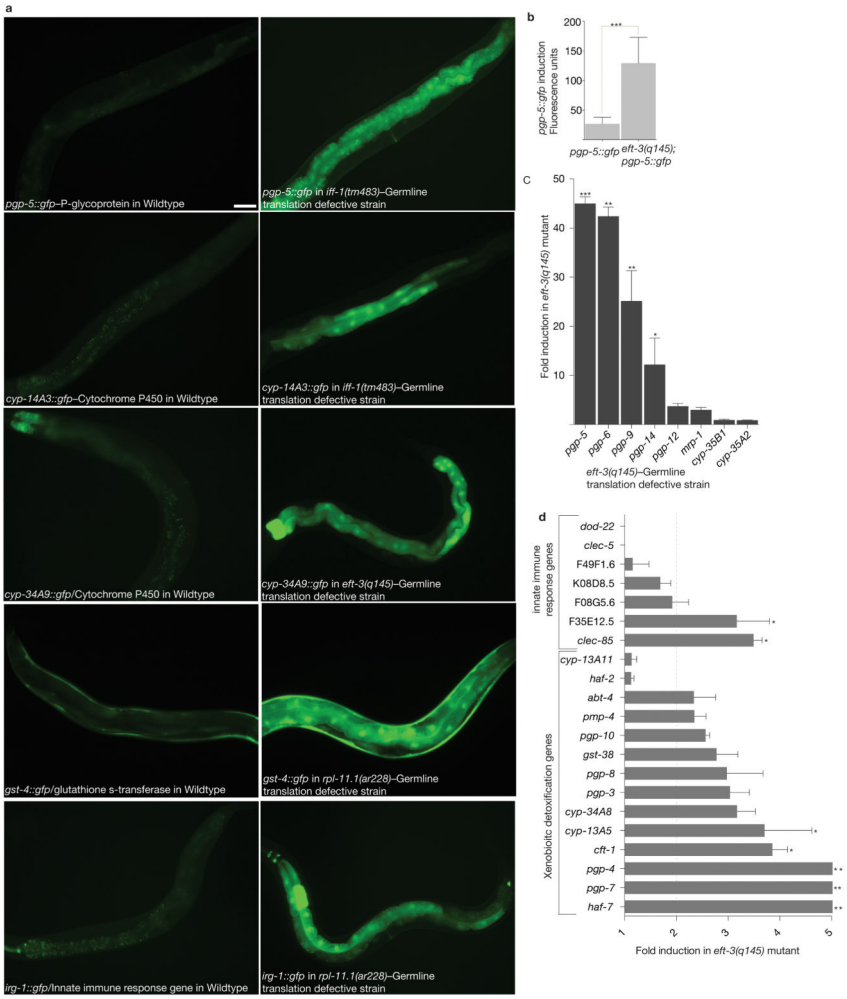

Figure 2. Translation defects in the germline induce systemic xenobiotic detoxification response

A) Genetic defects in germline translation induce xenobiotic and innate immune response GFP fusion genes. *iff-1*, *rpl-11.1*(ribosomal protein L11) and *eft-3* (an elongation factor 1-α ortholog) are expressed only in the germline and are required for translation in the germline only; they are not expressed in somatic cells or required for somatic translation[7]. Scale bar, 50 μm.

B) Quantification of *pgp-5::gfp* activation by germline translation defects. Fluorescence was measured using a COPAS Biosort. Unpaired t test; ***P<0.001. Mean ± s.d of n=413 and 1680 worms for *pgp-5::gfp*, and *eft-3 (q145); pgp-5::gfp* respectively. Data was consolidated from two independent experiments.

C) Genetic defects in germline translation induce xenobiotic efflux pump expression, as measured using PCR-based quantitation of mRNA levels of endogenous genes. Fold change compared to wildtype animals. Unpaired t test; ***P<0.001. **P<0.01. *P<0.05. ~300 worms per condition were washed off 1 plate for each experiment. Mean ± s.d from n=3 independent experiments is shown.

D) Genetic defects in germline translation induce xenobiotic and innate immune response genes, as measured using PCR-based quantitation of mRNA levels of endogenous genes.

Fold change compared to wildtype animals. Statistical significance was determined using unpaired t test. **P<0.01. *P<0.05. ~300 worms per condition were washed off 1 plate for each experiment. Mean ± s.d from n=3 independent experiments is shown.

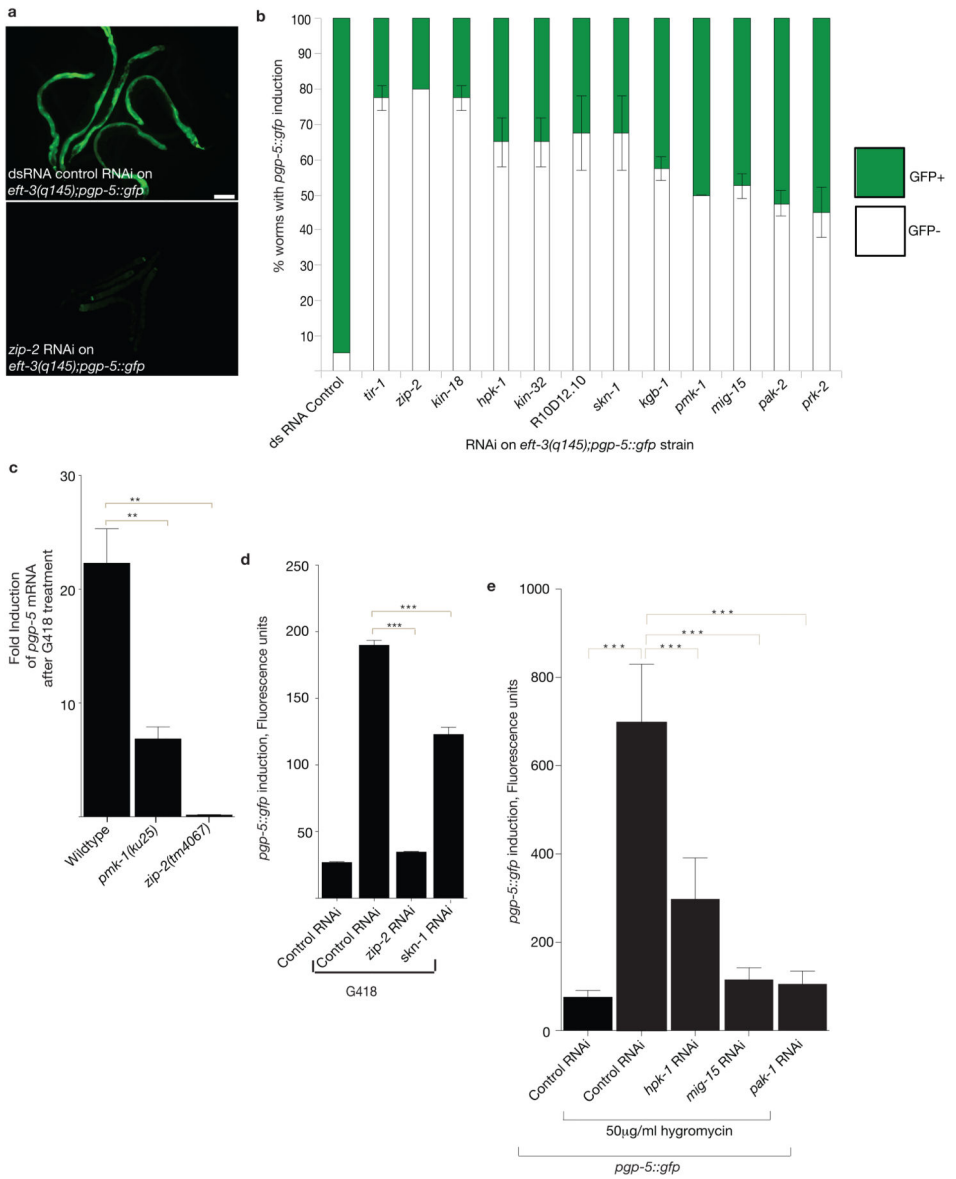

Figure 3. p38 MAPK signaling and *zip-2*–bZIP transcription factor are required for translation-inhibition-induced xenobiotic defense response

A) RNAi of the *zip-2–bZIP* transcription factor gene disrupts the induction of *pgp-5::gfp* in response to germline translation defects in *eft-3(q145);pgp-5::gfp*. Scale bar, 50μm.

B) Kinase and transcription factor gene inactivations that disrupt *pgp-5::gfp* induction in response to germline translation defects in the *eft-3(q145);pgp-5::gfp* strain. n=60 worms. Mean ± s.d. n is consolidated from three independent experiments.

C) p38–*pmk-1* and *zip-2* are required for G418 induction of *pgp-5* mRNA as assessed by qRT-PCR. Fold change compared to no drug wildtype animals. One-way ANOVA; **P<0.01. ~300 worms per condition were washed off 1 plate for each experiment. Mean ± s.d from n=3 independent experiments is shown.

D) *zip-2* and *skn-1* transcription factors are required for G418-induced *pgp-5::gfp* expression. Fluorescence was measured using a COPAS Biosort. Statistical significance was

determined using one-way ANOVA. ***P<0.001. Mean ± s.e.m of n=400 worms for control RNAi and n=399, 563, and 99 worms, respectively for G418 in combination with dsRNA control, *zip-2 RNAi* and *skn-1 RNAi* treatments. Data was consolidated from two independent experiments.

E) *hpk-1*,*mig-15*,and *pak-1* are required for hygromycin-induced induction of *pgp-5::gfp*. One-way ANOVA; ***P<0.001. Mean ± s.d. of n=136 worms for control RNAi and n=397, 268,123, 143 worms respectively for hygromycin treatment in combination with control RNAi, *hpk-1* RNAi, *mig-15 RNAi* and *pak-1 RNAi*. Data was consolidated from two independent experiments.

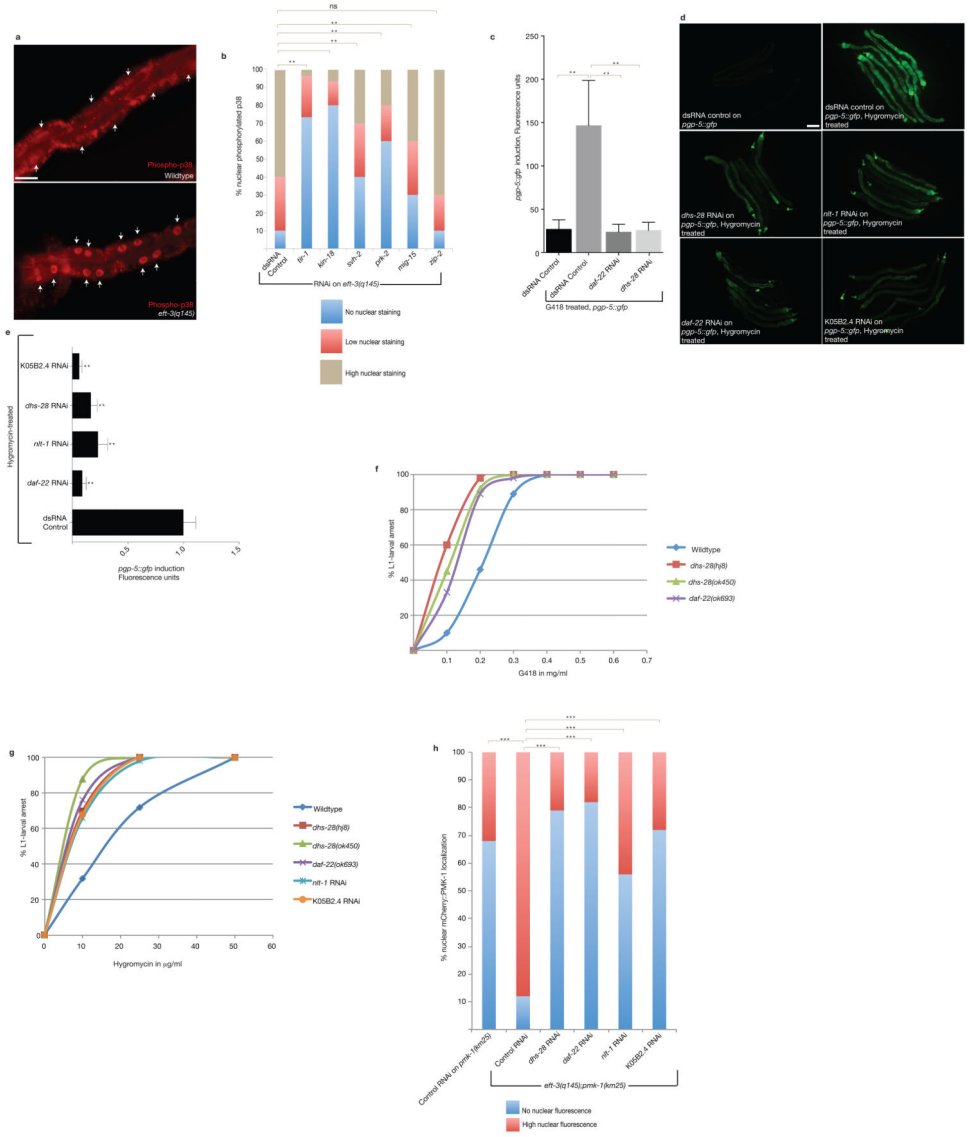

Figure 4. Bile acid-like biosynthetic signaling is required for translation-defective-induced xenobiotic defense response

A) Germline translation defects in the *eft-3(q145);pgp-5::gfp* strain causes p38 MAPK phosphorylation and nuclear translocation of active p38 PMK-1 in the intestine. Arrows indicate the nucleus. Scale bar, 20µm.

B) *tir-1*, *kin-18*, *svh-2*, *mig-15*,and *prk-2* are required for germline translation-defect-induced activation of p38 in the intestine. One-way ANOVA; **P<0.01. ns, P>0.05. n=50 (dsRNA control),45 (*tir-1 RNAi*), 50 (*kin-18 RNAi*),28 (*svh-2 RNAi*), 40 (*prk-2 RNAi*), 50 (*mig-15 RNAi*) and 32 (*zip-2 RNAi*) nuclei, respectively. Data represent one out of two independent experiments.

C) Inactivation of lipid and bile acid biosynthetic genes disrupts the induction of *pgp-5::gfp* in response to G418. Error bars represent SD. One-way ANOVA; **P<0.01. n=413 (dsRNA control non-G418 treated), n=2271(dsRNA control G418 treated), n=239 (*daf-22*

RNAi),n=514 (*dhs-28 RNAi*) worms. Data was consolidated from two independent experiments.

D) Lipid and bile acid biosynthetic genes are required for hygromycin-induced *pgp-5::gfp*. Scale bar, 50μm.

E) Inactivation of genes required for lipid–bile acid biosynthesis disrupts the induction of *pgp-5::gfp* in response to hygromycin. Error bars represent SD. One-way ANOVA; **P<0.01. n=10 worms for each condition. Data represent one out of two independent experiments.

F) While about 40% of control RNAi treated wildtype animals treated with 0.2 mg/ml G418 grew to adulthood, RNAi of *daf-22* and *dhs-28* cause >70% of animals treated with 0.2 mg/ml G418 to arrest at L1-larval stage. n=20 worms for each condition. Data represent one out of two independent experiments.

G) Mutations in genes required for lipid–bile acid biosynthesis cause hypersensitivity to G418. n=20 worms for each condition. Data represent one out of two independent experiments.

H) Lipid and bile acid biosynthetic genes are required for germline translation-defective-induced p38 nuclear localization. One-way ANOVA; ***P<0.001. n=50 nuclei (control RNAi on *pmk-1 (km25)*) and n=42 (control RNAi),32 (*dhs-28 RNAi*), 18 (*daf-22 RNAi*), 35 (*nlt-1RNAi*), and 50 (K05B2.4 RNAi) intestinal nuclei, respectively for *eft-3 (q145); pmk-1 (km25)*. Data represent one out of two independent experiments.

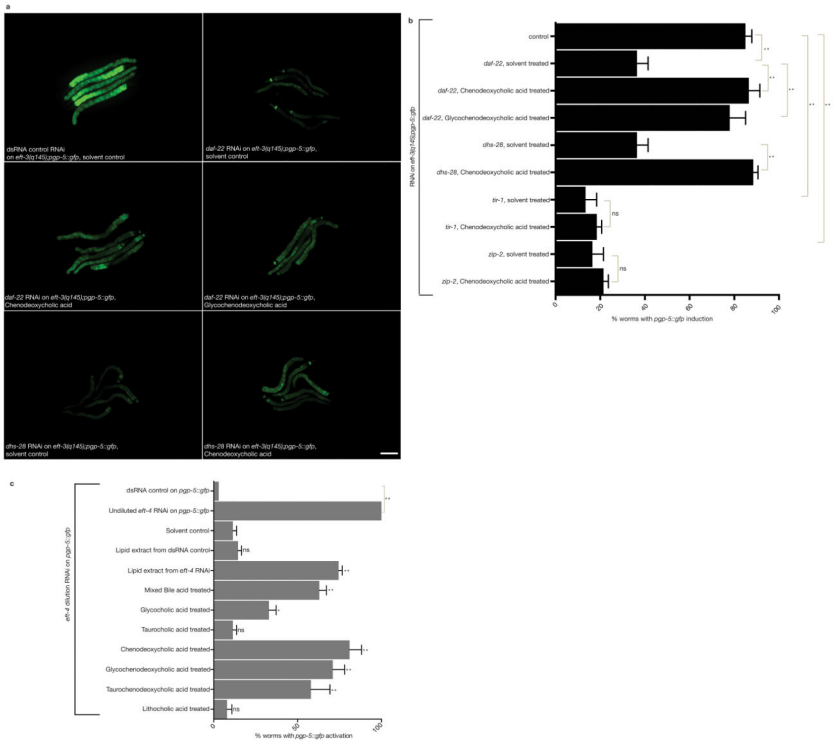

Figure 5. Bile acid signaling couples translation defects to the induction of xenobiotic defense genes

A) Mammalian bile acids rescue the defect in *pgp-5::gfp* induction caused by *daf-22* or *dhs-28* bile biosynthetic gene inactivations in the *eft-3(q145);pgp-5::gfp* strain with a germline translation elongation factor mutation. Scale bar, 50μm.

B) Quantitation of the rescue by mammalian bile acids of the defect in *pgp-5::gfp* induction caused by RNAi inactivation of *C. elegans* lipid–bile acid biosynthetic genes. Error bars represent SD. One-way ANOVA; *P<0.01. ns, P>0.05. n=100 worms. Data represent one out of three independent experiments.

C) Exogenous bile acids or lipid extracts from translationally-challenged *C. elegans* enhance the induction of *pgp-5::gfp* expression in response to mild translational inhibition by diluted *eft-4* RNA. Data are from two independent experimental replicates. N=100 worms. Error bars represent SD. Statistical significance was calculated by comparing to solvent control treated animals on eft-4 dilution RNAi using one-way ANOVA. **P<0.01. ns, P>0.05. Data represent one out of three independent experiments.

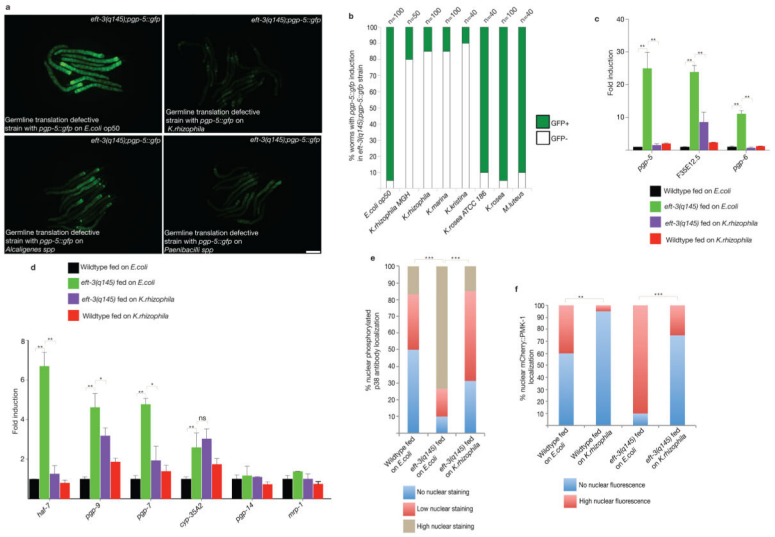

Figure 6. Bacterial suppression of the induction of xenobiotic responses by a germline-translation mutation

A) *C. elegans* grown on lawns of *Paenibacilli*, *Kocuria* or *Alcaligenes* bacteria fail to induce *pgp-5::gfp* in response to the germline-translation-defects in *eft-3(q145);pgp-5::gfp*. Scale bar, 50 μm.

B) *C. elegans* grown on various *Kocuria* species fail to induce *pgp-5::gfp* in response to the germline translation defects in *eft-3(q145);pgp-5::gfp*. Data represent one of two independent experiments. n denotes number of worms.

C) *C. elegans* grown on *K.rhizophila* fail to induce *pgp-5* and *pgp-6* in response to germline translation defects in *eft-3(q145)*. Error bars represent SD. Unpaired t test; **P<0.01. ~300 worms per condition were washed off 1 plate for each experiment. Mean ± s.d is from n=3 independent experiments.

D) *C. elegans* grown on *K.rhizophila* fail to induce various chromosomal xenobiotic and innate immune response genes in response to germline translation defects in *eft-3(q145)*. Error bars represent SD. Unpaired t test; **P<0.01. *P<0.05. ns, not significant. ~300 worms per condition were washed off 1 plate for each experiment. Mean ± s.d, n=3 independent experiments.

E) Feeding on *K.rhizophila* disrupts both basal and constitutive p38 MAPK phosphorylation as assessed using an antibody that recognizes active phosphorylated PMK-1 protein. One-way ANOVA. ***P<0.001. For wildtype on *E.coli*, n=20, for *eft-3(q145)* n=32 (*E.coli*) and 40 (*K. rhizophila*) nuclei, respectively. Data represent one out of two independent experiments.

F) Feeding on *K.rhizophila* disrupts the nuclear translocation of active phosphorylated p38 MAPK. Unpaired t test.. ***P<0.001. **P<0.01. For wildtype, n=50 (*E.coli*) 40 (*K.rhizophila*) nuclei, and for *eft-3 (q145)* n=55 (*E.coli*) and 48 (*K. rhizophila*) nuclei, respectively. Data represent one of two independent experiments.